

Adsorption of uranium from aqueous solution using HDTMA⁺-pillared bentonite: isotherm, kinetic and thermodynamic aspects

You-Qun Wang · Zhi-bin Zhang · Qin Li · Yun-Hai Liu

Received: 11 January 2012 / Published online: 5 February 2012
© Akadémiai Kiadó, Budapest, Hungary 2012

Abstract The ability of hexadecyltrimethylammonium cation pillared bentonite (HDTMA⁺-bentonite) has been explored for the removal and recovery of uranium from aqueous solutions. The adsorbent was characterized using small-angle X-ray diffraction, high resolution transmission electron microscopy, and Fourier transform infrared spectroscopy. The influences of different experimental parameters such as solution pH, initial uranium concentration, contact time, dosage and temperature on adsorption were investigated. The HDTMA⁺-bentonite exhibited the highest uranium sorption capacity at initial pH of 6.0 and at 80 min. Adsorption kinetics was better described by the pseudo-second-order model and adsorption process could be well defined by the Langmuir isotherm. The thermodynamic parameters, ΔG° (308 K), ΔH° , and ΔS° were determined to be -31.64 , -83.84 kJ/mol, and -169.49 J/mol/K, respectively, which demonstrated the sorption process of HDTMA⁺-bentonite towards U(VI) was feasible, spontaneous, and exothermic in nature. The adsorption on HDTMA⁺-bentonite was more favor than Na-bentonite,

in addition the saturated monolayer sorption capacity increased from 65.02 to 106.38 mg/g at 298 K after HDTMA⁺ pillaring. Complete removal ($\approx 100\%$) of U(VI) from 1.0 L simulated nuclear industry wastewater containing 10.0 mg U(VI) ions was possible with 1.5 g HDTMA⁺-bentonite.

Keywords Hexadecyltrimethylammonium bromide · Bentonite · Adsorption · Uranium

Introduction

Uranium is a toxic and weakly radioactive heavy metal exists in the environment ubiquitously, such as rocks, soils, and waters [1]. Therefore, the removal and recovery of uranium from contaminated surface and ground water, as a result of nuclear industries, has attracted more and more attention [2–4].

Several methods are available for removing uranium from aqueous solution, such as chemical precipitation [5], reverse osmosis [6], solvent extraction [7], micellar ultrafiltration [8, 9], and adsorption. Among these, adsorption is an attractive method due to its high efficiency, ease of handling, and availability of different adsorbents. Various kinds of new adsorbents for removing and recovering uranium have been reported [10–12], among which natural clays and their composites are considered as particularly effective, low-cost, and chemical stability. Bentonite is a well-defined naturally occurring 2:1 aluminosilicate mineral consisting of one alumina octahedral layer sandwiched between two silica tetrahedral layers. The potential adsorption sites for metal ions on bentonite include silanol ($\equiv \text{SiOH}$) and aluminol ($\equiv \text{AlOH}$), hydroxyl groups on the mineral edges and the permanently charged ($\equiv \text{X}^-$) on the

Y.-Q. Wang · Z. Zhang · Q. Li · Y.-H. Liu
Key Laboratory of Radioactive Geology and Exploration
Technology Fundamental Science for National Defense,
East China Institute of Technology, Fuzhou 344000,
People's Republic of China

Y.-Q. Wang · Z. Zhang · Q. Li · Y.-H. Liu
Department of Chemistry, Biological and Materials Sciences,
East China Institute of Technology, Fuzhou 344000,
People's Republic of China

Z. Zhang (✉) · Y.-H. Liu
State Key Laboratory Breeding Base of Nuclear Resources and
Environment (East China Institute of Technology), Ministry of
Education, Nanchang 330013, People's Republic of China
e-mail: zhangnjut@163.com

basal surfaces. The adsorption properties of bentonite can be improved by surface modification, such as the pillaring of certain metal oxides and polymeric species into interlayers, results in an increase in basal spacing, surface area and pore volume, which produces a structure with 2D micropores. The application of pillared clays for environmental pollution control in terms of metal removal from aqueous media has received much attention [13–17]. There among, HDTMA⁺-pillared bentonite is used to remove heavy metal ions, such as Pb²⁺, Pd²⁺, Cd²⁺, Zn²⁺ and Cr⁶⁺ from aqueous solution, whereas relatively minor attention is paid to UO₂²⁺ sorption [18–22]. Majdan et al. [21, 22] proposed the relationship between uranium sorption capacity with the amount of HDTMA⁺ cation loading in bentonite, in addition the possible species of uranium adsorbed on the surface.

In this paper, sodium bentonite was modified by hexadecyltrimethylammonium bromide (HDTMAB) to obtain a more efficient sorbent. Various techniques were used to characterize the structure and textural property of HDTMA cation pillared bentonite (HDTMA⁺-bentonite), including small-angle X-ray diffraction (SAXRD), high resolution transmission electron microscopy (HRTEM) and Fourier transform infrared spectroscopy (FTIR). The effect of various experimental parameters including pH of the solution, contact time, initial uranium concentration, dose of sorbent, and temperature, as well as adsorption kinetics, isotherm models, and thermodynamics were investigated.

Materials and methods

Materials

Sodium bentonite (Na-bentonite) was purchased from Zhejiang Fenghong Clay Chemicals Co., Ltd., and the cation exchange capacity (CEC) was 100 mmol/100 g bentonite. For the preparation of a stock uranium(VI) solution, 1.1792 g U₃O₈ was put into a 100 mL beaker, and 10 mL hydrochloric acid ($\rho = 1.18$ g/mL), 2 mL 30% hydrogen peroxide were added. The solution was heated until it was nearly dry and then 10 mL hydrochloric acid ($\rho = 1.18$ g/mL) was added. The solution was transferred to a 1,000 mL volumetric flask and diluted to the mark with distilled water to produce U(VI) stock solution (1 mg/mL). The uranium solutions were prepared by diluting the stock solution to appropriate volumes depending upon the experimental requirements. All other reagents were of AR grade.

Preparation of HDTMA⁺-bentonite

Five grams of Na-bentonite was swelled by 100 mL distilled water, then HDTMAB solution was slowly added to bentonite suspension followed by stirring at 60 °C for 24 h

to obtain HDTMA⁺-bentonite with HDTMAB to the CEC of bentonite molar ratios of 1.0:1, 1.2:1, 1.3:1, 1.4:1, 1.5:1, and 1.6:1 (labeled as 1.0CEC-bentonite, 1.2CEC-bentonite, 1.3CEC-bentonite, 1.4CEC-bentonite, 1.5CEC-bentonite, and 1.6CEC-bentonite), respectively. The suspension was filtered and was washed with deionized water until a negative bromide test had been obtained with 0.1 M AgNO₃, and then dried at 60 °C for 12 h. All samples were ground and sieved to 200 mesh size.

Characterization

Small-angle X-ray diffraction patterns were recorded using Cu K α radiation ($\gamma = 1.5418$) on ARL X'TRA diffractometer operating at 40 kV and 40 mA with 0.25° divergence slit and 0.5° anti-scatter slit between 1.0° and 16° (2θ) at a step size of 2°/min. High resolution transmission electron microscopy (HRTEM) was carried out using a Jeol 4010 operated at 400 kV. The IR spectra were recorded as KBr pellets in the spectral range of 400–4,000 cm⁻¹ on Nicolet Nexus 870 Fourier transform infrared spectrometer.

Adsorption experiments

The adsorption of U(VI) was studied as a function of pH, contact time, initial uranium concentration and temperature. The batch sorption was performed in a reciprocating water bath shaker with concussion speed of 200 rpm. In the experiments 0.01 g of sorbent was suspended in 50 mL solution containing different U(VI) concentration and different initial pH (adjusted with 0.1 mol/L HNO₃ and 0.1 mol/L NaOH). The concentration of U(VI) in the solution was determined by the arsenazo(III) method with a 721 type spectrophotometer at 650 nm [23]. The amount of uranyl ions adsorbed per unit mass of the bentonite was calculated by using expression 1:

$$q_e = \frac{(C_0 - C_e)V}{W} \quad (1)$$

where q_e is the adsorption capacity of the bentonite (mg/g), C_0 and C_e are the uranium concentration in the initial and equilibrium solution (mg/L) respectively, V is the volume of the aqueous solution (L) and W is the mass of dry bentonite (g).

Results and discussion

Characterization

The SAXRD patterns of Na-MMT and HDTMA-MMT was shown in Fig. 1, and the interlayer spacing could be calculated by Eq. 2.

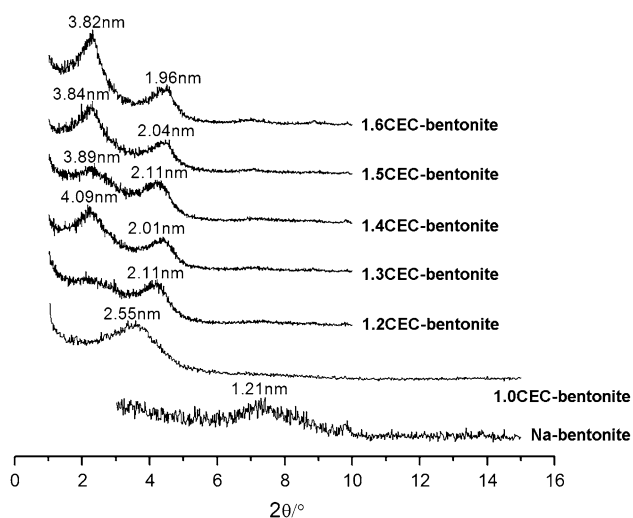


Fig. 1 Small-angle X-ray diffraction patterns of Na-bentonite and HDTMA⁺-bentonite (1.0CEC-bentonite to 1.6CEC-bentonite were HDTMA⁺:CEC of 1.0:1, 1.2:1, 1.3, 1.4:1, 1.5:1 and 1.6:1 respectively)

$$d = \frac{n\lambda}{2 \sin \theta} \quad (2)$$

where the d is the interlayer spacing (nm), θ is the diffraction angle ($^{\circ}$) and the λ is 0.154 nm.

The d_{001} value of Na-bentonite was 1.21 nm and expanded gradually to 4.09 nm with pillared by HDTMA⁺. These results indicate that HDTMA⁺ cations had been intercalated into the bentonite interlayer space. Based on the molecular structure of HDTMA⁺ and the interlayer spacing, different HDTMA⁺ arrangement models within the bentonite interlayer space are proposed, i.e., lateral-monolayer in 1.0CEC-bentonite and 1.2 CEC-bentonite, lateral-monolayer and lateral-bilayer in 1.3CEC-bentonite, 1.4CEC-bentonite and 1.5 CEC-bentonite, lateral-monolayer (or pseudo-trilayer) and lateral-bilayer in 1.6CEC-bentonite.

Fig. 3 TEM image of 1.3CEC-bentonite

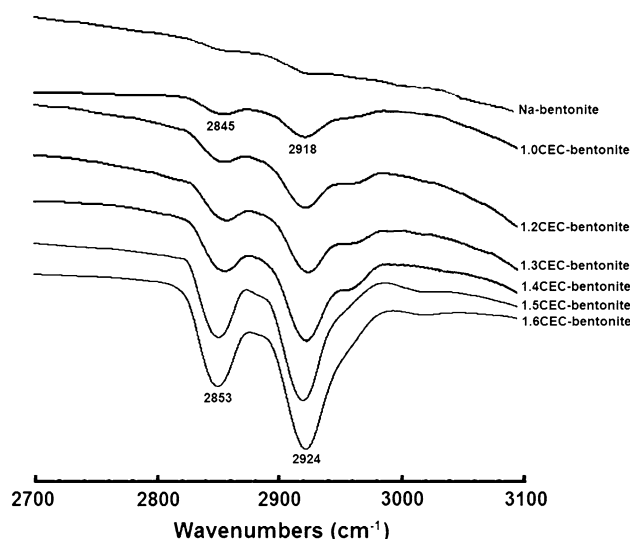
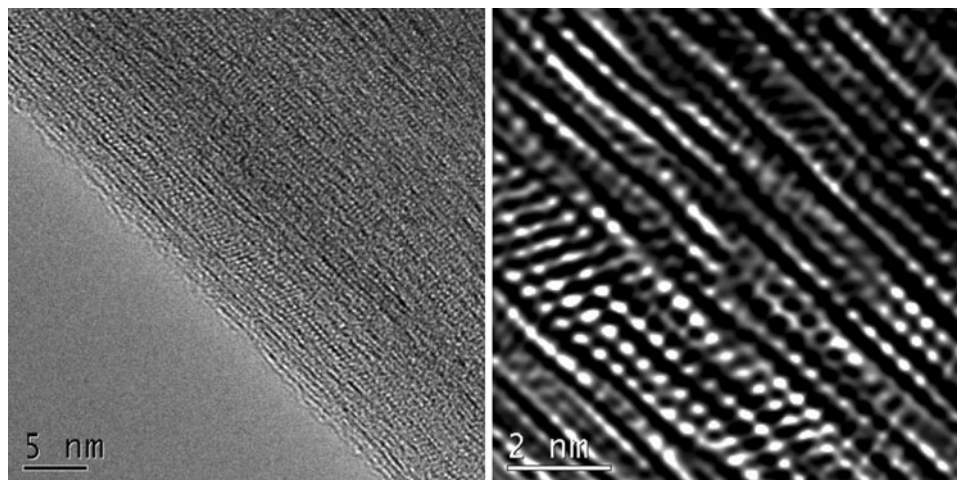


Fig. 2 FTIR spectra of Na-bentonite and HDTMA⁺-bentonite (2,700–3,100 cm^{-1})

Figure 2 shows the FTIR spectra of the HDTMA⁺-bentonite composites in the range of 2,700–3,100 cm^{-1} . As shown in Fig. 2, the intensities of the two intense adsorption bands at about 2,850 and 2,920 cm^{-1} , corresponding to the anti-symmetric and symmetric CH_2 stretching modes of amine, respectively, increase gradually with increase of the packing density of amine chains within the bentonite galleries. The HDTMA⁺-bentonite with HDTMA⁺:CEC of 1.3 was used to investigate the sorption properties towards uranium in the following experiments.

The HRTEM images of 1.3CEC-bentonite were shown in Fig. 3, from which, it could be seen that the interlamellar structure bentonite was still maintained after pillared by HDTMA⁺ and the interlayer space was expanded. However, the arrangement model of HDTMA⁺ was a mix state and there were several arrangements coexist in the interlayer.

The effect of solution pH

The pH of solution is one of the most crucial parameters for the sorption of metal ions. It can affect the surface charge, the metal speciation, and surface metal binding sites. The effect of pH on the adsorption of U(VI) onto Na-bentonite and HDTMA⁺-bentonite was carried out over the pH range 3.0–8.0 using 50 µg/mL initial uranium concentration at 298 K and the results were displayed in Fig. 4. The adsorption of U(VI) on Na-bentonite and HDTMA⁺-bentonite was greatly depended on the variation of solution pH. As for Na-bentonite, the amounts of uptake were increased from 3.0 to 5.0, and reached the maximum adsorption capacity of 58.3 mg/g at pH 5.0 and then declined after 5.0. While for HDTMA⁺-bentonite, the adsorption of U(VI) was increased with the solution pH from 3.0 to 6.0 and obtained the maximum adsorption capacity of 82.5 mg/g and then declined after 6.0. The low adsorption capacity at lower pH value could be attributed to the increasing positivity of the adsorbents and the competition of H⁺ ions with U(VI) on the adsorptive active sites. And with the increase of pH above 6, the hydroxide products of U(VI), such as UO₂(OH)⁺, (UO₂)₂(OH)₂, and (UO₂)₃(OH)₅²⁺ appeared and led to the decrease of the adsorption capacity [24]. Therefore, the solution pH of 5 and 6 was used for the further experiments for U(VI) adsorption on Na-bentonite and HDTMA⁺-bentonite, respectively.

The effect of contact time

Contact time is also an important factor which can reflect the adsorption kinetics. The variation of adsorption amount with vibrating time was studied using 50 µg/mL initial U(VI) concentration at pH 6.0 and 298 K. As showed in Fig. 5, the amount of U(VI) adsorbed on Na-bentonite and

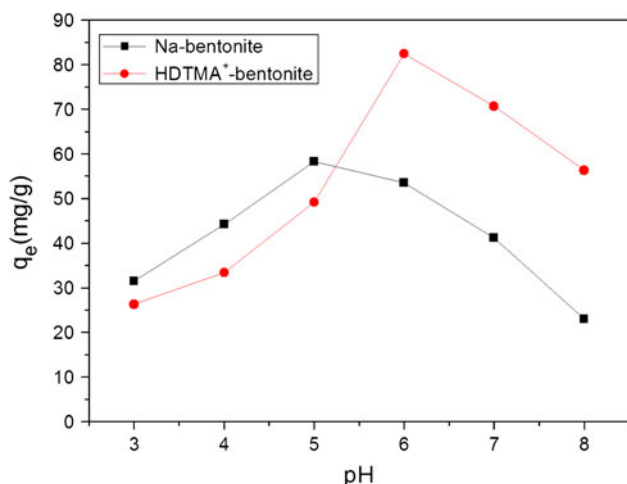


Fig. 4 The effect of solution pH on U(VI) adsorption on Na-bentonite and HDTMA⁺-bentonite

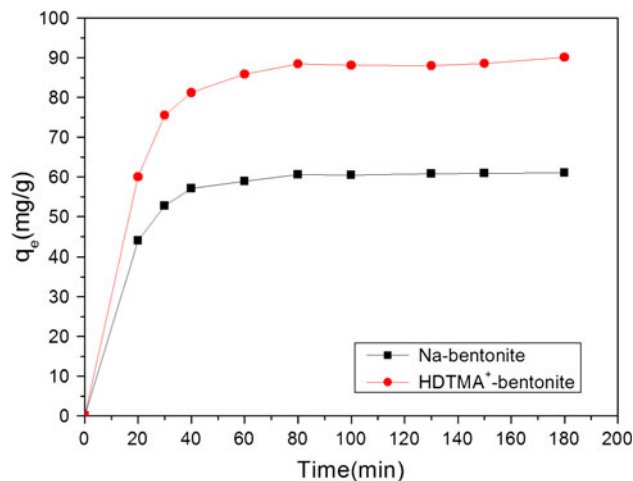


Fig. 5 The effect of contact time on U(VI) adsorption on Na-bentonite and HDTMA⁺-bentonite

HDTMA⁺-bentonite increased sharply at the beginning, and then gradually reached equilibrium after 80 min. The faster adsorption rate at the beginning would be due to the larger concentration gradient. Therefore, the contact time of 80 min was deemed sufficient to establish sorption equilibrium and used in all subsequent experiments.

The effect of initial U(VI) concentration

The initial concentration provides an important driving force to overcome all mass transfer resistance of uranium between the aqueous and solid phases [25]. The effect of initial U(VI) concentration on sorption was studied at 298 K and revealed in Fig. 6. The adsorptive capacity increased with the increase of the initial U(VI) concentration. According to the actual situation, the concentration of uranium in next following experiments should be controlled at 50 µg/mL.

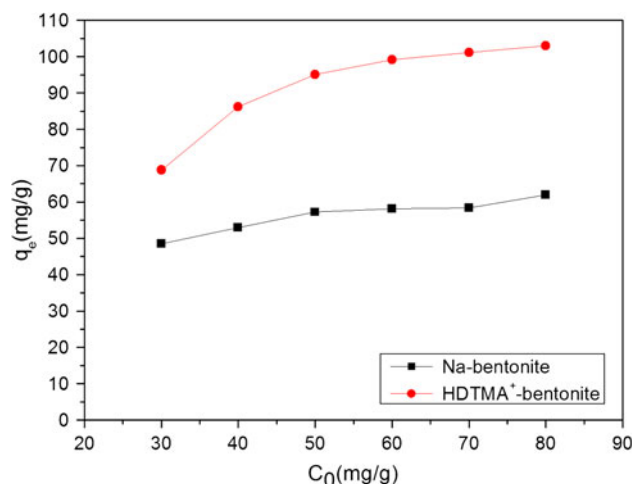


Fig. 6 The effect of initial concentrations on U(VI) adsorption on Na-bentonite and HDTMA⁺-bentonite

Adsorption isotherm

The equilibrium adsorption isotherms are one of the essential data to understand the mechanism of the adsorption systems. Langmuir and Freundlich equations are the most frequently used for describing sorption isotherms. The Langmuir model is based on assumptions of adsorption homogeneity such as equally available adsorption sites, monolayer surface coverage, and no interaction between adsorbed species. The Langmuir equation can be described by the linearized Eq. 3 [26].

$$\frac{C_e}{q_e} = \frac{1}{q_m K_L} + \frac{C_e}{q_m} \tag{3}$$

where C_e is the equilibrium concentration (mg/L), q_e is the amount of solute sorbed per unit weight of sorbent (mg/g), q_m is the Langmuir constant, which represents the saturated monolayer sorption capacity (mg/g). K_L is a constant related to the energy of adsorption.

The Freundlich model can be applied to nonideal sorption on heterogeneous surfaces as well as multilayer sorption [27]. The empirical Freundlich equation can also be transformed into linearized Eq. 4.

$$\ln q_e = \ln K_F + \frac{1}{n} \ln C_e \tag{4}$$

where C_e is the equilibrium concentration (mg/L), q_e is the amount of solute sorbed per unit weight of sorbent (mg/g), K_F is the Freundlich constant related to the adsorption capacity, and n is relevant to the adsorption intensity.

Figures 7, 8 present the effect of initial concentration on the uranium adsorption on Na-bentonite and HDTMA⁺-bentonite at 298, 308, and 318 K.

The linearized form of Langmuir and Freundlich adsorption isotherms obtained at 298, 308, and 318 K were

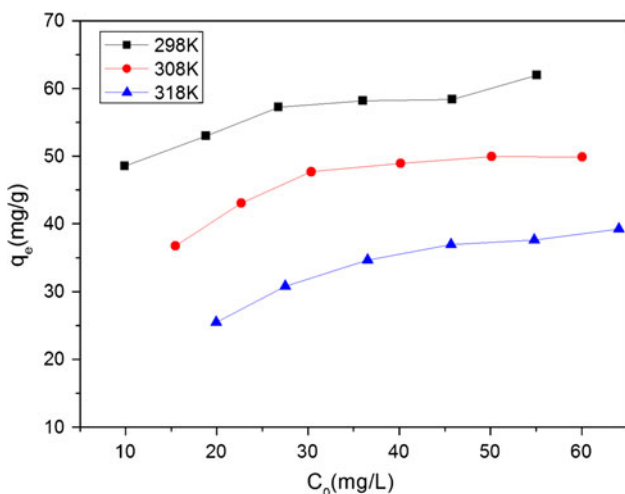


Fig. 7 The adsorption isotherms of Na-bentonite at 298, 308, and 318 K

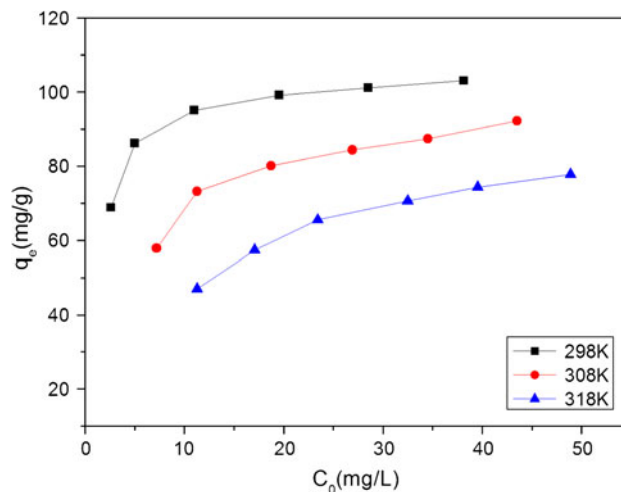


Fig. 8 The adsorption isotherms of HDTMA⁺-bentonite at 298, 308, and 318 K

presented in Figs. 9, 10, 11, and 12, respectively. And the adsorption constants evaluated from the isotherms with the correlation coefficients (R^2) were given in Table 1. The value of R^2 showed that Langmuir isotherm model fitted better with the experimental data than Freundlich isotherm model. Moreover, the saturated monolayer sorption capacity (q_m) increased from 65.02 to 106.38 mg/g at 298 K after HDTMA⁺ pillaring. A larger value of K_L also implies strong bonding of uranium to HDTMA⁺-bentonite. Furthermore, with the increase of the temperature, the saturated monolayer sorption capacity decreased for the same adsorbents, which indicated the sorption of U(VI) is exothermic.

Adsorption kinetics

In order to explain the controlling mechanism of adsorption processes, such as mass transfer and chemical reaction,

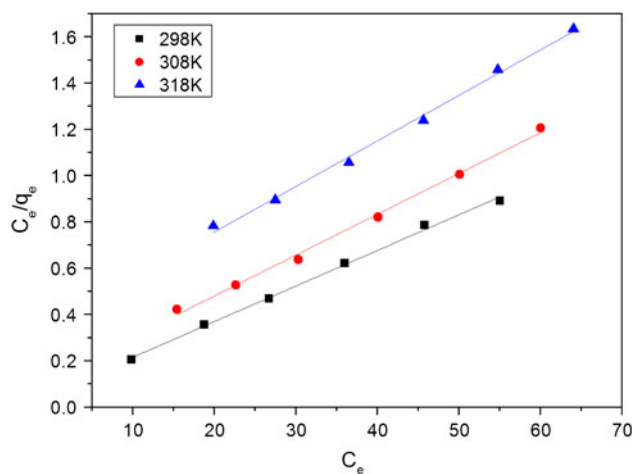


Fig. 9 The Langmuir adsorption isotherms of Na-bentonite

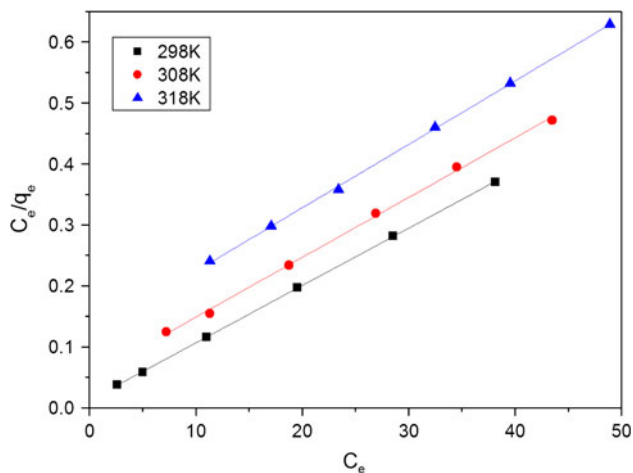


Fig. 10 The Langmuir adsorption isotherms of HDTMA⁺-bentonite

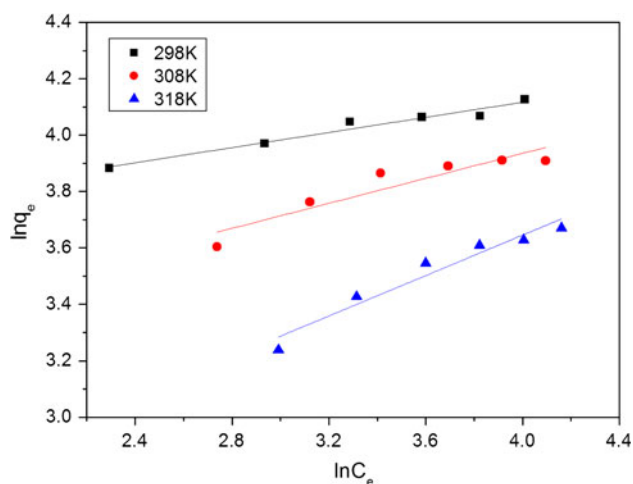


Fig. 11 Freundlich isotherms of the Na-bentonite

pseudo-first-order, and pseudo-second-order kinetic equations were applied to describe the kinetic characteristic of U(VI) onto the bentonite. The pseudo-first order kinetic model is usually given as Eq. 5 [28].

$$\ln(q_e - q_t) = \ln q_e - k_1 t \quad (5)$$

where k_1 (min^{-1}) is the rate constant of first order adsorption, q_e and q_t are the amounts of U(VI) adsorbed (mg/g) at equilibrium and time “ t ”, respectively. Using Eq. 5, linear plot of $\ln(q_e - q_t)$ vs. “ t ” was plotted (Fig. 13). The k_1 , $q_{e,\text{cal}}$ and R^2 were calculated from the plot and presented in Table 2.

The pseudo-second order kinetic model is always given as Eq. 6 [29].

$$\frac{t}{q_t} = \frac{1}{k_2 q_e^2} + \frac{t}{q_e} \quad (6)$$

where k_2 (min^{-1}) is the rate constant of second order adsorption. Using Eq. 6, linear plot of t/q_t vs. t was plotted

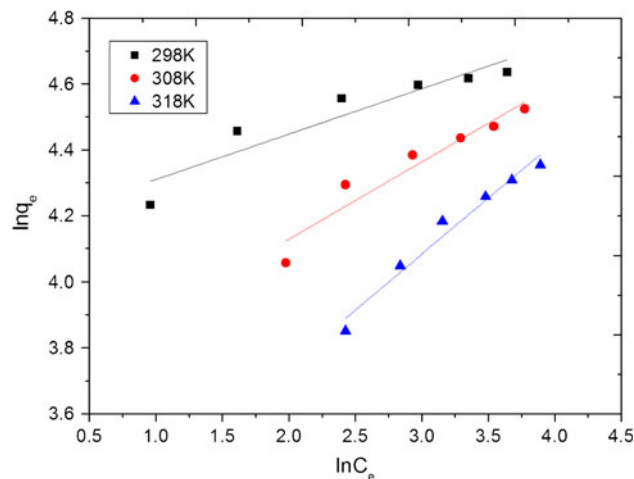


Fig. 12 Freundlich isotherms of the HDTMA⁺-bentonite

(Fig. 14). The k_2 , $q_{e,\text{cal}}$ and R^2 were calculated from the plot and presented in Table 2.

As showed in Table 2, the square of R^2 of pseudo-second order equation was better than the value of the pseudo-first order equation. Moreover, the values of the amounts of U(VI) adsorbed at equilibrium, $q_{e,\text{cal}}$ (63.41, 93.90 mg/g) was very close to the experimental values, $q_{e,\text{exp}}$ (60.63 and 88.47 mg/g). Therefore, the adsorption process is more favor of the pseudo-second order equation, which indicate that adsorption involves chemical reaction in adsorption in addition to physical adsorption [30].

Adsorption thermodynamics

Thermodynamic parameters such as enthalpy (ΔH°), entropy (ΔS°), and Gibbs free energy (ΔG°) are useful in defining whether the sorption reaction is endothermic or exothermic, and spontaneity of the adsorption process [31]. The thermodynamic data were calculated using the following Eqs. 7 and 8.

$$\ln k_L = \frac{\Delta S^\circ}{R} - \frac{\Delta H^\circ}{RT} \quad (7)$$

$$\Delta G^\circ = \Delta H^\circ - T\Delta S^\circ \quad (8)$$

where k_L is the Langmuir constant, ΔS° is the change of entropy (J/mol/K), ΔH° is the change of enthalpy (kJ/mol), T is the absolute temperature in Kelvin (K) and R is the gas constant (8.314 J/mol/K). ΔH° and ΔS° can be calculated from the slope and intercept of the straight line (Fig. 15). The change of Gibbs free energy values are calculated from Eq. 8.

The values of thermodynamic parameters for the sorption of U(VI) at different temperature were given in Table 3. The negative value of ΔG° at different temperatures confirmed the feasibility and spontaneous nature of adsorption process. Further, the increase in the value ΔG°

Table 1 Isotherm constants and R^2 for the adsorption of U(VI) on bentonite

Adsorbents	T (K)	Langmuir isotherm			Freundlich isotherm		
		K_L	q_m (mg/g)	R^2	n	K_F	R^2
Na-bentonite	298	0.26	65.02	0.9968	7.45	35.87	0.9514
	308	0.14	56.69	0.9952	4.51	21.08	0.8359
	318	0.05	50.79	0.9943	2.79	9.13	0.9330
HDTMA ⁺ -bentonite	298	0.75	106.38	0.9999	7.25	64.83	0.8515
	308	0.19	101.94	0.9981	4.25	38.77	0.9055
	318	0.09	96.15	0.9994	2.96	21.52	0.9636

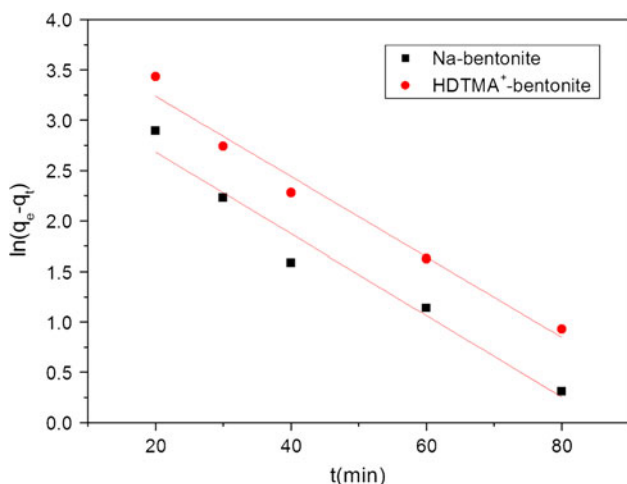


Fig. 13 The pseudo-first order adsorption kinetics

with the increasing temperature indicated that lower temperature favored the sorption process. In addition, the ΔG° value of HDTMA⁺-bentonite was smaller than the Na-bentonite, which showed the adsorption on HDTMA⁺-bentonite was more favor than Na-bentonite. The negative value of ΔS° reflected the affinity of the bentonite for U(VI) and confirmed the decreased randomness at the solid-solution interface during adsorption [32].

Test with simulated nuclear industry wastewater

The simulated U(VI) nuclear industry wastewater was recovered by HDTMA⁺-bentonite to demonstrate its adsorption potential and utility in removing U(VI) ion from wastewater in the presence of other ions. The wastewater was prepared according to the composition of resin adsorption tail liquid from uranium hydrometallurgy plant.

Table 2 Adsorption kinetics of Na-bentonite and HDTMA⁺-bentonite

Adsorbents	Pseudo-first order kinetics			Pseudo-second order kinetics		
	k_1 (min ⁻¹)	$q_{e,cal}$ (mg/g)	R^2	k_2 (g/mg/min)	$q_{e,cal}$ (mg/g)	R^2
Na-bentonite	0.040	32.87	0.9530	0.0027	63.41	0.9991
HDTMA ⁺ -bentonite	0.039	56.53	0.9713	0.0014	93.90	0.9986

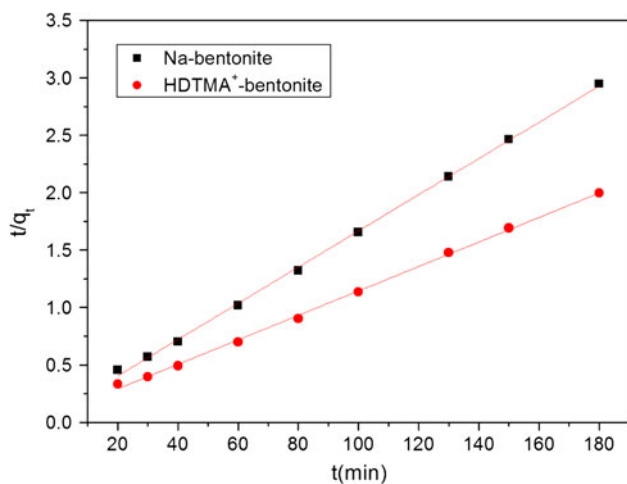


Fig. 14 Pseudo-second order adsorption kinetics

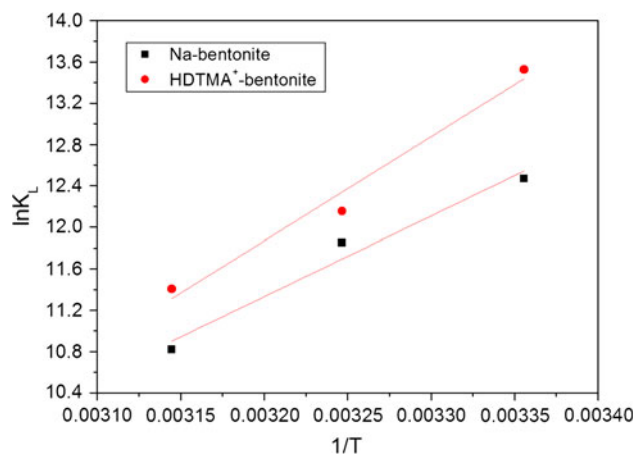
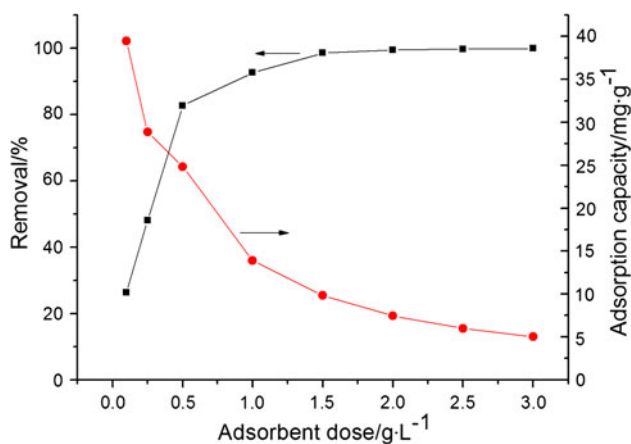


Fig. 15 The adsorption thermodynamics of U(VI) on Na-bentonite and HDTMA⁺-bentonite

Table 3 Thermodynamic parameters for the U(VI) sorption on Na-bentonite and HDTMA⁺-bentonite

Adsorbents	ΔG° (kJ/mol)			ΔH° (kJ/mol)	ΔS° (J/mol/K)
	298 K	308 K	318 K		
Na-bentonite	-31.11	-29.98	-28.85	-64.81	-113.10
HDTMA ⁺ -bentonite	-33.34	-31.64	-29.95	-83.84	-169.49

The wastewater contained U(VI) (15 mg/L), SO₄²⁻ (10 g/L), NO₃⁻ (1 g/L), Mg²⁺ (0.2 g/L), Ca²⁺ (0.5 g/L), and Fe³⁺ (1.6 g/L). The effect of adsorbent dose on U(VI) removal from wastewater was investigated (Fig. 16). The percentage of U(VI) adsorption increases with increasing HDTMA⁺-bentonite dosage and almost complete removal ($\approx 100\%$) of U(VI) from the wastewater containing 15 mg/L was achieved with 2.0 g HDTMA⁺-bentonite in 1.0 L.

**Fig. 16** U(VI) ion removal from simulated nuclear industry wastewater by HDTMA⁺-bentonite

U(VI) sorption capacity and cost comparison of HDTMA⁺-bentonite with other natural clays and their composites

The U(VI) sorption capacity and cost of HDTMA⁺-bentonite were compared with other natural clays and their composites, as showed in Table 4, the cost of Na-bentonite was 0.12–0.15 US \$/kg, and the whole cost of HDTMAB and the pillaring process for 1.0 kg Na-bentonite was 0.80 US \$. Thus, the cost of HDTMA⁺-bentonite (0.92–0.95 US \$/kg) was much cheaper than some other adsorbents, such as Na-rectorite, MPDET-kaolinite and commercial activated carbon. However, the U(VI) sorption capacity of HDTMA⁺-bentonite (106.38 mg/g) was even larger than that of commercial activated carbon (93.10 mg/g). Obviously, HDTMA⁺-bentonite was a perfect adsorbent towards U(VI) with cheap price, large adsorption capacity and ease of handling.

Conclusions

In this paper, HDTMA cation pillared bentonite (HDTMA⁺-bentonite) was prepared. The interlayer spacing expanded gradually from 1.21 to 4.09 nm by HDTMA⁺ pillaring. The HDTMA⁺ loading amount increased with the increase of HDTMAB:CEC of bentonite during preparation. The

Table 4 Sorption capacity and cost comparison of HDTMA⁺-bentonite with other adsorbents

Adsorbents	Sorption properties			Price/US \$/kg	Reference
	pH	Time/min	Sorption capacity/mg/g ^b		
Na-bentonite	5.0	60	65.02	0.12–0.15	This work
HDTMA ⁺ -bentonite	6.0	60	106.38	0.92–0.95	This work
Clinoptilolite zeolite	5.0	120	0.48	0.32–0.45	[33]
Na-attapulgit	6.5	300	6.04	0.14–0.85	[34]
Na-rectorite	≈ 7.0	150	16.93	1.50	[35]
Kaolinite	4.0	10	0.77	0.13–0.20	[36]
MPDET-kaolinite ^a	4.0	10	1.28	1.80–2.00	[37]
Volcanic tuff	5.0	30	1.01	0.05–0.10	[38]
Commercial activated carbon	4.0	60	93.10	20.0–22.0	[39]

^a MPDET-kaolinite, *N*¹-[3-(trimethoxysilyl)propyl]diethylenetriamine was anchored onto Amazon kaolinite surface by heterogeneous route

^b Sorption capacity, the saturated monolayer sorption capacity calculated by Langmuir isotherm model

interlamellar structure of HDTMA⁺-bentonite was still maintained, however, the arrangement model of HDTMA⁺ was a mix state and there were several arrangements coexist in the interlayer. The sorption performances were controlled by solution pH, contact time, initial uranium concentration and sorbent dosage. The maximum capacity of HDTMA⁺-bentonite was observed at the pH value of 6.0 and at 80 min. The U(VI) sorption on HDTMA⁺-bentonite was well fitted to the Langmuir adsorption isothermal and pseudo-second kinetics models. The thermodynamic parameters, such as ΔG° , ΔH° , and ΔS° , clearly indicated that the adsorption process was feasible, spontaneous and exothermic in nature, in addition the adsorption on HDTMA⁺-bentonite was more favor than Na-bentonite. Attempts for removal of U(VI) from simulated nuclear industry wastewater using HDTMA⁺-bentonite revealed acceptability. Almost complete removal ($\approx 100\%$) of U(VI) from the wastewater containing 15 mg/L was achieved with 2.0 g HDTMA⁺-bentonite in 1.0 L.

Acknowledgments This work was financially supported by the National Natural Science Foundation of China (Grant No. 21101024), Key Project of Chinese Ministry of Education (Grant No. 211086), Natural Science Foundation of Jiangxi Province (No. 2010GQH0015), Science and Technology project of Jiangxi Provincial Department of Education (No. GJJ11139) and Open Project Foundation of the Key Laboratory of Radioactive Geology and Exploration Technology Fundamental Science for National Defense, East China Institute of Technology, China (2010RGET08).

References

- Jackson BP, Ranville JF, Bertsch PM, Sowder AG (2005) *Environ Sci Technol* 39:2478–2485
- Donia AM, Atia AA, Moussa EMM, El-Sherif AM, El-Magied MOA (2009) *Hydrometallurgy* 95:183–189
- Smith SC, Douglas M, Moore DA, Kukkadapu RK, Arey BW (2009) *Environ Sci Technol* 43:2341–2347
- Xie S, Zhang C, Zhou X, Yang J, Zhang X, Wang J (2009) *J Environ Radioact* 100:162–166
- Djedidi Z, Bouda M, Souissi MA, Ben Cheikh R, Mercier G, Tyagi RD, Blais JF (2009) *J Hazard Mater* 172:1372–1382
- Abdel-Khalek AA, Ali MM, Ashour RM, Abdel-Magied AF (2011) *J Radioanal Nucl Chem* 290:353–359
- Kumari N, Prabhu DR, Pathak PN, Kanekar AS, Manchanda VK (2011) *J Radioanal Nucl Chem* 289:835–843
- Cojocar C, Zakrzewska-Trznadel G, Jaworska A (2009) *J Hazard Mater* 169:599–609
- Cojocar C, Zakrzewska-Trznadel G, Miskiewicz A (2009) *J Hazard Mater* 169:610–620
- Li X, Song Q, Liu B, Liu C, Wang H, Geng J, Chen Z, Liu N, Li S (2011) *Prog Chem* 23:1446–1453
- Sprynskyy M, Kowalkowski T, Tutu H, Cukrowska EM, Buszewski B (2011) *Chem Eng J* 171:1185–1193
- Hussein AEM (2011) *J Radioanal Nucl Chem* 289:321–329
- Zhao HT, Jaynes WF, Vance GF (1996) *Chemosphere* 33:2089–2100
- Huh JK, Song DI, Jeon YW (2000) *Sep Sci Technol* 35:243–259
- Upson R, Burns S (2006) *J Colloid Interface Sci* 297:70–76
- Hsu YH, Wang MK, Pai CW, Wang YS (2000) *Appl Clay Sci* 16:147–159
- Dentel SK, Jamrah AI, Sparks DL (1998) *Water Res* 32:3689–3697
- Lee JJ, Choi J, Park JW (2002) *Chemosphere* 49:1309–1315
- Oyanedel-Craver VA, Fuller M, Smith JA (2007) *J Colloid Interface Sci* 309:485–492
- Akar ST, Yetimoglu Y, Gedikbey T (2009) *Desalination* 244:97–108
- Majdan M, Pikus S, Gajowiak A, Gładysz-Płaska A, Krzyżanowska H, Żuk J, Bujacka M (2010) *Appl Surf Sci* 256:5416–5421
- Majdan M, Pikus S, Gajowiak A, Sternik D, Zieba E (2010) *J Hazard Mater* 184:662–670
- Liu Y, Cao X, Hua R, Wang Y, Liu Y, Pang C, Wang Y (2010) *Hydrometallurgy* 104:150–155
- Bayramoglu G, Celik G, Arica M (2006) *J Hazard Mater* 136:345–353
- Aytas S, Yurtlu M, Donat R (2009) *J Hazard Mater* 172:667–674
- Hazer O, Kartal Ş (2010) *Talanta* 82:1974–1979
- Parab H, Joshi S, Shenoy N, Verma R, Lali A, Sudersanan M (2005) *Bioresour Technol* 96:1241–1248
- Ghaemi A, Torab-Mostaedi M, Ghannadi-Maragheh M (2011) *J Hazard Mater* 190:916–921
- Psareva T, Zakutevskyy O, Chubar N, Strelko V, Shaposhnikova T, Carvalho J, Correia M (2005) *Colloid Surf A* 252:231–236
- Anirudhan TS, Rijith S, Tharun AR (2010) *Colloid Surf A* 368:13–22
- Anirudhan TS, Divya L, Suchithra PS (2009) *J Environ Manag* 90:549–560
- Donat RJ (2009) *Chem Thermodyn* 41:829–835
- Kilincarslan A, Akyil S (2005) *J Radioanal Nucl Chem* 264(3):541–548
- Zhu W, Liu Z, Chen L, Dong Y (2011) *J Radioanal Nucl Chem* 289(3):781–788
- Zhao D, Yang S, Chen S, Guo Z, Yang X (2011) *J Radioanal Nucl Chem* 287(2):557–565
- Gao L, Yang Z, Shi K, Wang X, Guo Z, Wu W (2010) *J Radioanal Nucl Chem* 284(3):519–526
- Guerra DL, Leidens VL, Viana RR, Airoidi C (2010) *J Solid State Chem* 183(5):1141–1149
- Yusan S, Aslani MAA, Turkozu DA, Aycan HA, Aytas S, Akyil S (2010) *J Radioanal Nucl Chem* 283(1):231–238
- Mellah A, Chegrouche S, Barkat M (2006) *J Colloid Interface Sci* 296(2):434–441